Carbohydrate Polymers 370 (2025) 124378

Contents lists available at ScienceDirect

Carbohydrate Polymers

journal homepage: www.elsevier.com/locate/carbpol

Comparative analysis of supplemental irrigation effects on structure and digestion of normal and amylose-only barley starches

Wenxin Liang [a,b], Klaus Herburger [a], Ke Guo [b,j], Jacob Judas Kain Kirkensgaard [c,d], Kim Henrik Hebelstrup [e,f], Staffan Persson [b,g], Sheng Chen [h,i], Yuyue Zhong [i], Andreas Blennow [k,*], Li Ding [b,i,**]

[a] Institute of Biological Sciences, University of Rostock, Germany
[b] Department of Plant and Environmental Sciences, Faculty of Science, University of Copenhagen, Denmark
[c] Department of Food Science, University of Copenhagen, DK-1958, Frederiksberg C, Denmark
[d] Niels Bohr Institute, Universitetsparken 5, 2100, København Ø, Denmark
[e] Department of Agroecology, Aarhus University, Flakkebjerg, Denmark
[f] Plantcarb ApS, Hørsholm, Denmark
[g] Joint International Research Laboratory of Metabolic & Developmental Sciences, State Key Laboratory of Hybrid Rice, SJTU-University of Adelaide Joint Centre for Agriculture and Health, School of Life Sciences and Biotechnology, Shanghai Jiao Tong University, Shanghai, China
[h] State Key Lab of Chemical Biology and Drug Discovery and the Department of Food Science and Nutrition, The Hong Kong Polytechnic University, Hung Hom, Kowloon, Hong Kong, China
[i] Department of Food Science and Nutrition, The Hong Kong Polytechnic University, Hung Hom, Kowloon, Hong Kong, China
[j] Institute of Food Crops, Jiangsu Academy of Agricultural Sciences, Nanjing, 210014, China
[k] Department of Biotechnology and Food Engineering, Guangdong Technion-Israel Institute of Technology, Shantou, 515063, China

ARTICLE INFO

Keywords:
Supplementary irrigation
Amylose-only starch
Barley
Starch biosynthesis
Resistant starch

ABSTRACT

To investigate the effects of supplemental irrigation (SI) on yield and starch quality in barley with different genotypes, a normal barley cultivar (NB) and an amylose-only mutant (AO) were cultivated under well-watered (WW) and SI conditions. Compared to WW, SI reduced grain yield by 1–4 % and starch content by 2–5 % in both genotypes, with a more pronounced reduction observed in NB than in AO. SI decreased photosynthetic capacity in NB but enhanced it in AO, consistent with observed differences in starch granule abundance in leaf tissues. SI increased the proportion of amylopectin long chains with degree of polymerization (DP) $>$ 36 in NB, while elevating amylose short chains with DP $\leq$ 24 in AO. In addition, SI led to upregulation of starch synthase IIa (*SSIIa*) in NB and downregulation of starch synthase I (*SSI*) and *SSIIa* in AO. SI also enhanced the content of rapidly digestible starch in NB by 3 % but slowly digestible starch in AO by 4.5 %. These findings indicated genotype-specific responses of barley to SI, providing novel insights into the impact of SI on yield and starch functionality across different barley genotypes.

1. Introduction

Barley (*Hordeum vulgare* L.) is the fourth most important cereal crop globally, particularly in Asia and northern Africa, where it is primarily cultivated for brewing and livestock feed (Asare et al., 2011). Water availability is a critical factor influencing barley growth, as droughts of varying durations and intensities can significantly reduce the grain yield (Samarah, Alqudah, Amayreh, & McAndrews, 2009). To mitigate drought-related yield losses, different irrigation methods are employed in barley cultivation. Flood and furrow irrigation are the most widely used conventional practices among farmers; however, these methods have low water use efficiency (WUE), leading to substantial water wastage, and increasing the risk of lodging and soil erosion (Fahong, Xuqing, & Sayre, 2004; Ippolito, Bjorneberg, Stott, & Karlen, 2017). In contrast, drip irrigation, increases water efficiency but is costly and requires advanced technical expertise and management (Fonteyne, Flores García, & Verhulst, 2021). Therefore, the development of cost-effective and water-efficient irrigation methods is crucial for sustainable barley

* Corresponding author.
** Correspondence to: L. Ding, Department of Plant and Environmental Sciences, Faculty of Science, University of Copenhagen, Denmark.
E-mail addresses: andreas.blennow1@gmail.com (A. Blennow), liding952022@163.com (L. Ding).

https://doi.org/10.1016/j.carbpol.2025.124378
Received 12 June 2025; Received in revised form 6 September 2025; Accepted 9 September 2025
Available online 9 September 2025

production.

Supplemental irrigation (SI) is an advanced, cost-effective strategy aimed at enhancing water use efficiency (WUE) and addressing the limitations of conventional irrigation methods. SI optimizes irrigation by supplying water based on plant-specific needs during critical growth stages, as demonstrated in crops such as wheat (Liang et al., 2021). This method relies on measuring soil moisture content to determine the appropriate irrigation levels during key developmental stages. Previous studies have shown that SI significantly increased yield and WUE in winter wheat (Guo, Yu, Wang, Shi, & Zhang, 2014; Wang, Yu, & White, 2013), lentil (Oweis, Hachum, & Pala, 2004), maize (Jian et al., 2024) and potato (Gowing & Ejieji, 2001). For example, Jian et al. (2024) applied SI to maize under heat stress and observed increased grain sink capacity, a prolonged effective grain-filling period by 1.4–6.5 days, a higher average filling rate (14.8–41.0 %), and increased grain yield (15.8–22.3 %). Starch, a major component of many main crops, plays a crucial role in determining the viscosity, texture, mouthfeel, and digestibility of crop-based foods (Ding et al., 2023). However, most SI studies focus on plant growth and yield, with few research on its effects on starch quality. Notably, our previous study indicated that SI reduced amylose (AM) content, decreased the proportion of amylopectin (AP) chains with a degree of polymerization (DP) of 13–24, and lowered relative crystallinity, while it increased the proportions of AP chains with DP 6–12 and 25–36, as well as induced formation of more B-type granules in winter wheat (Liang et al., 2021). However, this investigation was limited to a single starch genotype, highlighting a significant gap in the understanding about the effects of SI on diverse starch varieties, particularly genetically engineered ones. Addressing this gap is essential for optimizing SI practices to improve WUE and promote the sustainability of genotype-specific crop production.

Given the homologous genome architectures and comparable chromosomal counts of wheat and barley, we hypothesized that SI modulates yield and starch quality compared to conventional irrigation methods, and different barley genotypes exhibit distinct responses to SI. To test how SI affects the yield and starch qualities in different genotypes, two barley genotypes were selected: normal barley (NB), an elite cultivar, and its engineered AM-only (AO) variant with suppression of expression of all starch branching enzyme (*SBE*) genes, which has significant potential for producing low-glycemic foods and bioplastics (Carciofi et al., 2012). NB and AO are near-isogenic lines, sharing an identical genomic background except for the *SBE* gene silencing, resulting in dramatic changes in the AM contents (32 % *vs* 97 %). Two irrigation treatments, including SI and well-watered (WW), were applied, and their effects on plant growth, grain yield, starch structure, and expression of starch synthetic genes were analyzed. Compared to our previously studied wheat (Liang et al., 2021), barley serves as a complementary model due to its simpler genome and distinctive starch metabolic traits, particularly the availability of well-characterized and unique AO mutants. Pure AM starch has only been reported in barley, making it a unique model for characterizing the effects of SI on both the yield and starch quality of AM-only starch. Additionally, the altered carbon partitioning and source-sink dynamics in AO provide a valuable framework for investigating how genotypes with distinct starch metabolic backgrounds respond to different irrigation methods, and, although AO was not intentionally bred for drought resistance, its unique physiological profile will offer important insights into how starch metabolic pathways influence water use dynamics. By including the AO barley genotype, the findings of this study will broaden the understanding of SI effects across different crops, rather than focusing solely on wheat.

2. Materials and methods

2.1. Materials

Isoamylase (*E*-ISAMY, 200 units/mL), pullulanase (EPULBL, 1000 units/mL), and total starch assay kit were bought from Megazyme (K-TSTA, Megazyme, Co. Wicklow, Ireland). Pancreatin from porcine pancreas (Cat. No. P7545, 8 × USP) and amyloglucosidase (Cat. No. A7095, 300 unit/mL) were purchased from Sigma-Aldrich Chemical Co. (St. Louis, MO, USA). All other chemicals used in this study were of analytical grade.

2.2. Experimental site and crop management

2.2.1. Experimental setup

The plants were grown in a greenhouse at the University of Copenhagen, Denmark, from January to the end of June 2020, resulting in a total growth period of approximately five months. Two barley cultivars were used: normal barley (NB, cv. Golden Promise, 32 % AM content) and AM-only (AO, 97 % AM content, a transgenic line derived from the Golden Promise genetic background, where all *SBE* homologues are suppressed *via* RNA interference, leading to the presence of only AM fraction, as determined by size exclusion chromatography (Carciofi et al., 2012)).

2.2.2. Irrigation treatments

The irrigation treatments were conducted under controlled greenhouse conditions to minimize environmental variation and isolate genotype x irrigation interactions. Two irrigation treatments were applied: WW (control) and SI. The selection of WW treatment as the control rather than a drought treatment was to isolate the effects of SI without introducing severe stress, which could obscure starch-related responses. The experiment consisted of 48 potted barley plants, divided into four groups: NB + WW, NB + SI, AO + WW, and AO + SI, with each group containing 12 pots. Each pot held three barley plants, all grown in identical pots with standardized soil. To ensure uniform experimental conditions and minimize environmental bias, pot positions were rotated daily, maintaining consistent exposure to light, temperature, and humidity.

Watering treatments began at the three-leaf growth stage and continued until the end of the grain-filling stage. Initially, the soil was saturated to its field capacity (FC) by allowing excess water to drain, and the corresponding pot weight was recorded as 100 % FC. To regulate irrigation, a soil moisture threshold was established based on a percentage of FC: 85 % for WW treatment and 70 % for the SI treatment. The rationale for setting these two thresholds is that, in pot experiments, maintaining soil moisture at 85 % FC ensures an optimal balance between air and water availability in the root zone, thereby supporting healthy plant growth (Passioura, 2006); in contrast, when soil moisture falls below 70 % FC, barley growth is adversely affected. Further, soil moisture levels were monitored by weighing the pots before and after watering. When the weight of a pot fell below these thresholds, water was added to restore it to the designated level. Both treatments were monitored every other day, with water supplementation made as needed to maintain the target soil moisture content, ensuring accurate comparison between the two irrigation regimes.

2.3. Evaluation of growth process and total starch content

The growth stages of barley were monitored and recorded every other day to evaluate the duration of each phase. The full growth period was separated into seven distinct stages: emergence (17 days), tillering (23 days), jointing (30 days), booting (19 days for SI, and 20 days for WW), anthesis (5 days), grain filling (34 days for SI and 35 days for WW), and maturity stage. Tiller number, a key component affecting grain yield, was assessed on the first day of the anthesis stage. The first day of the anthesis stage was defined as the day when at least 50 % of the spikes on the main stem had visible extruded anthers, indicating active flowering. This occurred approximately on day 89 for SI and day 90 for WW, depending on the booting stage duration. This timing was selected because tillers present during anthesis typically develop into mature spikes. The number of spikes per plant was recorded at the maturity

stage. Three spikes from each barley plant were selected to determine the grain number per spike and grain yield. Additionally, the collected grains were used to measure the thousand-grain weight and total starch content and were stored for further starch extraction and characterization.

The total starch content was measured by using the Megazyme total starch assay kit (K-TSTA, Megazyme, Co. Wicklow, Ireland). Briefly, 10 mg barley flour, obtained from grinding barley grains, was mixed with 1 mL 80 % ethanol and heated at 99 °C for 30 min before centrifugation at 4000 *g* for 5 min. The supernatant was discarded and the precipitate was collected and mixed with 0.2 mL of dimethyl sulphoxide (DMSO) while stirring. The sample was heated at 99 °C for 5 min and digested with 0.3 mL of thermostable α-amylase (3000 U/mL) at 99 °C for 12 min while stirring. The sample was cooled to 50 °C, and 0.4 mL of sodium acetate buffer (200 mM, pH 4.5) containing calcium chloride (5 mM) and 0.01 mL amyloglucosidase (3300 U/mL) were added and incubated for 30 min while shaking, followed by centrifuging at 4000 g for 10 min. The supernatant (0.05 mL) was tested for glucose content using the Megazyme GOPOD kit.

2.4. Visualization of leaf starch

Barley flag leaves were harvested on the first day of the anthesis stage (day 89 for SI and day 90 for WW) and soaked in 10 mL portions of 80 % ethanol at 80 °C until no green leaf pigmentation was visible. Starch was stained with Lugol's solution (0.37 % iodine and 0.74 % potassium iodide). Stained leaves were visualized using an Olympus BX41 light microscope equipped with an Olympus UPLFLN 40× objective (numerical aperture 0.5) and a GXCAM LITE (GT Instruments).

2.5. Photosynthesis rate of leaves

The photosynthetic performance of barley leaves was measured on the first day of the anthesis stage using a Li-6400 photosynthesis instrument. Net photosynthetic carbon assimilation (μmol CO_2 m^{-2} s^{-1}) was used as a proxy. The measurement started at 8:30 AM, and leaves of the four treatments were measured every 2 h from 8:30 AM to 6:30 PM. For each treatment, ten healthy and intact leaves were selected and measured at five time points during the day. The same set of leaves was used across all time points for consistency. Light intensity was set to match natural sunlight at the light saturation point (1200 μmol photons m^{-2} s^{-1}, and measurements were adjusted for variable external conditions. If the external light intensity turned out to be insufficient, the light induction was performed first, followed by measurement of CO_2 assimilation. The weaker the external light intensity, the longer the light induction time.

2.6. Starch extraction and apparent AM content (AAC)

Starch was extracted from barley flour using a previous method as described (Goldstein et al., 2016). Briefly, barley grains were ground to a fine powder and starch granule intactness was monitored by light microscopy. Next, 20 g barley flour was vigorously mixed with 20 mL 0.5 % SDS (sodium dodecyl sulphate) and 100 mM DTT (dithiothreitol) and incubated for 30 min while mixing, ensuring that all the flour was suspended uniformly. Starch granules were sedimented in a 4 °C refrigerator overnight, centrifuged and the supernatant was discarded without disturbing the pellet. Sedimentation and centrifugation were repeated three times. Deionized water was added to remove the SDS and the DTT reductant and to separate the lipids from the starch. The resulting slurry was passed through a 100-μm sieve and the starch was dried at 40 °C and the starch granules gently dispersed.

The measurement of AAC of the barley starches was performed as described (Wickramasinghe, Blennow, & Noda, 2009). Five starch samples with known AC (0 %, 2.1 %, 26 %, 30 % and 40 %) were used as AM standards. 5 mg of starch samples was mixed with 0.75 mL of 4 M NaOH, and incubated overnight at room temperature with continuous shaking at 800 rpm. A 10 μL aliquot of the fourfold diluted solution was then mixed with 200 μL of Lugol's iodine solution. Absorbance was measured at 550 nm and 620 nm using a microplate reader, and the AAC was calculated based on a standard curve.

2.7. High-performance anion-exchange chromatography with pulsed amperometric detection (HPAEC-PAD)

Starch samples (5 %, *w*/w in 0.05 M acetate buffer with pH of 4) were heated at 99 °C for 1 h and debranched by isoamylase at 40 °C for 3 h. The resulting linear malto-oligosaccharides (40 μL, 5 mg/mL) were separated by an HPAEC-PAD (Dionex, Sunnyvale, CA, USA). The peak integration and detector response were performed as described (Blennow, Bay-Smidt, Wischmann, Olsen, & Møller, 1998). The relative contents of 4 chain-length fractions were then calculated and denoted: fa (DP 6–12), fb1 (DP 13–24), fb2 (DP 25–36), and fb3 (DP >36).

2.8. Proton nuclear magnetic resonance (^{1}H NMR) spectroscopy

The degree of branching of starch was determined using one-dimensional ^{1}H NMR spectra acquired on 600 MHz NMR spectrometers (Bruker Avance III; Bruker Biospin, Rheinstetten, Germany), following a previous protocol (Zhong et al., 2021) with some modifications. Briefly, starch samples (5 %, *w*/w) were gelatinized at 99 °C for 1 h in deuterium oxide and lyophilized. The freeze-dried samples were re-dissolved in 1 mL of 9:1 (*v*/v) DMSO containing 1.0 mg/mL 3-(Trimethylsilyl) propionic-2,2,3,3d4 acid sodium salt (TSP) in deuterium oxide by heating at 100 °C for 30 min, and 0.7 mL of the supernatant was transferred into NMR glass tubes with 178 mm length and 5.0 mm diameter. Data were collected by one-dimensional ^{1}H signal NMR spectroscopy at 60 °C.

2.9. Wide-angle X-ray scattering analysis (WAXS)

The crystalline structures of starch samples were measured with a Nano-inXider instrument (Xenocs SAS, Grenoble, France) equipped with a Cu Kα source with a 1.54 Å wavelength and a two-detector setup according to the method described previously(Zhong, Keeratiburana, et al., 2021). The samples, equilibrated at approximately 90 % relative humidity, were enclosed within mica films with a thickness of 5–7 μm before analysis. The X-ray diffractogram was then recorded through a diffraction angle 2θ range of 5–35°. The total relative crystallinity was calculated as the ratio between crystalline peak area to the total diffraction area by PeakFit software (Version 4.0, Systat Software Inc., San Jose, CA, USA).

2.10. Fourier transform infrared (FTIR) spectroscopy

The starch granular surface structure ordering was analyzed using a Bomem MB100 FTIR spectrometer (ABB-Bomem, Quebec, Canada), equipped with an ATR single reflectance cell containing a germanium crystal (Thermo Fisher Scientific, Hudson, USA). The original spectra were corrected by subtracting the baseline (800–1200 cm^{-1}) before deconvolution using OMNIC software (Thermo Fisher Scientific, USA). The line shape was assumed to be Lorentzian, with a bandwidth of 70.4 cm^{-1} and a resolution enhancement factor of 2.0 (Song et al., 2020).

2.11. Scanning electron microscopy (SEM)

The starch granular morphology was evaluated using an FEI Quanta 200 field emission scanning electron microscope (FE-SEM). Starch granules were fixed, sputter-coated with gold, and images were taken at an acceleration voltage of 2 kV at 2000× magnification.

2.12. Granule size distribution

The size distribution of the starch granules was measured with a laser diffraction particle size analyzer (Microtrac S3500, Florida, USA) according to the manufacturer's instructions.

2.13. In vitro digestion

In vitro digestion of starch was measured as described (Liang et al., 2023) with modifications. Starch (100 mg, uncooked or cooked at 100 °C for 20 min) was suspended in 5 mL water in 50 mL polypropylene centrifuge tubes containing 5 glass beads. The tubes were capped and vortexed for 5 min. After adding 10 mL sodium acetate buffer (0.1 M, pH 5.2), the dispersion was incubated horizontally in a shaking water bath at 37 °C for 30 min. Pancreatin (18.75 mg) and amyloglucosidase (13.4 μL) prepared in 2.5 mL sodium acetate buffer were added to each tube. Aliquots (0.1 mL) were taken after 20 min and 120 min and mixed with 1 mL of 95 % ethanol to terminate the reaction, and the glucose content in the mixture was measured with the Megazyme GOPOD kit following centrifugation at 5000 *g* for 10 min. The percentage of hydrolyzed starch was calculated from released glucose. The contents of rapidly digestible starch (RDS, within 20 min), slowly digestible starch (SDS, digestible in 20–120 min), and resistant starch (RS, undigestible after 120 min) were calculated.

2.14. RNA isolation and quantitative real-time PCR (qRT-PCR) expression analysis

According to the manufacturer's instructions, the total RNA of different barley kernels from each treatment was extracted by an RNAprep Pure Plant Plus Kit (Tiangen, Beijing, China). The expression levels from 7 key starch synthetic genes were analyzed as reported before (Carciofi et al., 2012).

2.15. Statistical analysis

All experiments were performed in triplicate, and the results are presented as mean ± standard deviation (SD). Statistically significant differences ($p < 0.05$) were analyzed by Analysis of Variance (ANOVA) followed by Duncan's test using SPSS 25.0 software (SPSS, Inc. Chicago, IL, USA).

3. Results and discussion

3.1. Plant growth, tiller number, grain yield and total starch content

The full growth period of barley as shown in Fig. 1A indicated that water treatments started from tillering stage and ended at maturation stage. SI treatment had minimal effects on the early growth stages of both barley cultivars but accelerated anthesis onset and shortened the grain-filling period by 2 days compared to WW irrigation. Similar effects have been observed in wheat under drought stress (Yu et al., 2016). The soil moistures were set as 85 % FC and 70 % FC, respectively, for WW and SI. Adequate irrigation in WW treatment helps maintain plant functionality during grain filling, potentially extending this critical period and allowing more time for dry matter accumulation in the grain. In contrast, mild water stress in SI induces earlier senescence and accelerates grain filling, leading to earlier maturation, which shortens the crop cycle and enables an earlier harvest (Dietz, Zorb, & Geilfus, 2021). Tiller number, which refers to the number of shoots emerging from the

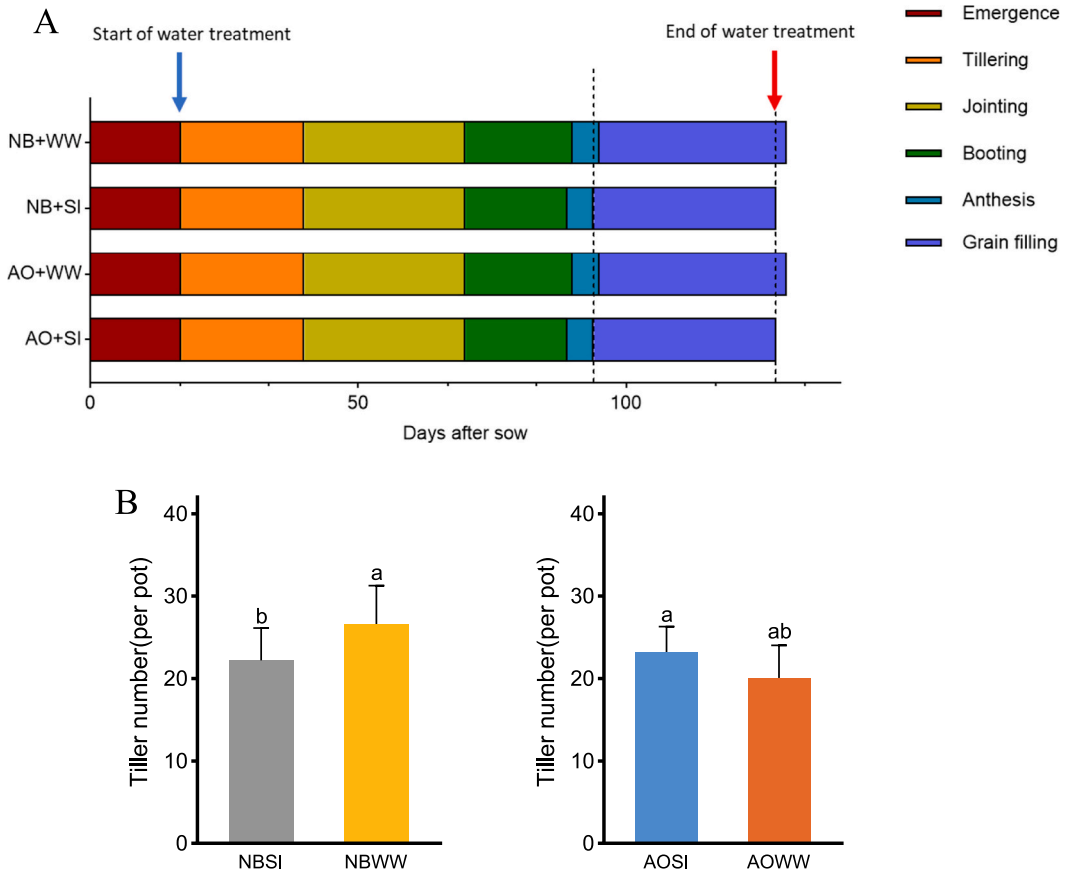

Fig. 1. The growth period (A), and tiller numbers (B) at anthesis stage of two barley genotypes subjected to two different irrigation methods (NB, Normal barley (wild type); AO, Amylose-only; SI, Supplemental irrigation; WW, Well-watered).

main stem or crown, is an important indicator of plant vigor and developmental dynamics in barley. As shown in Fig. 1B, NB plants under SI treatment exhibited slightly fewer tillers at anthesis compared to the WW condition, whereas AO showed the opposite trend, with a slightly higher tiller number under SI. Although these differences were not statistically significant, the divergent trends suggest genotype-specific responses to reduced irrigation, thereby supporting our hypothesis.

The yield and yield component data (Table 1) indicated that SI had no significant effect on the grain number per spike or thousand-grain weight in both barley genotypes, indicating that these yield components were preserved despite reduced irrigation. However, SI significantly reduced the number of spikes and grain yield per plant in NB, in line with its decreased tiller number. In contrast, SI only slightly decreased these parameters in AO, suggesting that NB is more sensitive to reduced irrigation than AO. A similar trend was observed in the total starch content (TSC) of barley grains (Table 1), where SI led to a greater reduction in NB than in AO. Similar reductions in yield and spike number under SI have been reported in winter wheat compared to traditional irrigation (Liang et al., 2021). Additionally, reduced irrigation in vetch resulted in fewer branches per plant and lower seed yield (Dogan, 2019). The reduced yield and starch content observed under SI treatment are closely associated with the two-day shortening of the grain-filling period as shown in Fig. 1A, indicating reduced irrigation results in loss in yield and starch content (Dai, Li, Zhang, Yan, & Li, 2016). The differing responses of the genotypes to SI suggest that AO, with suppression of all *SBE* genes, exhibits greater resistance to reduced irrigation compared to NB.

3.2. Leaf photosynthesis and starch granules at the anthesis stage

Flag-leaf photosynthesis throughout the initial anthesis day (8:30 AM - 6:30 PM) was analyzed. As shown in Fig. 1B, the overall photosynthetic activity of SI-treated NB was lower than that of NB under WW conditions, reflecting its reduced yield and TSC (Table 1). Photosynthesis serves as the primary source of energy for plant growth and development, directly influencing biomass accumulation, grain filling, and overall yield (Honda et al., 2021). In contrast, AO subjected to SI exhibited higher photosynthetic capacity throughout the day compared to AO-WW. Although this increase in photosynthesis was expected to enhance the grain yield of AO, no significant improvements were observed. Carbon fixed during photosynthesis supports grain development and can be also stored as starch in leaves (Ambavaram et al., 2014). Therefore, leaf starch content was further visualized using iodine staining after ethanol washing. Data in Fig. 2B revealed that compared to NB, AO accumulated more starch in their leaves under both irrigation conditions. This result suggests that AO exhibits distinct source-sink regulation mechanisms, which leads to altered carbon allocation and water response patterns. Previous studies also indicated that the coordinated regulation of photosynthesis and assimilate allocation can indirectly influence plant responses to water stress (Ambavaram et al., 2014). SI treatment reduced starch accumulation in NB leaves while increasing it in AO leaves, which agrees with the photosynthetic data. These results further imply that in NB with lower resistance to reduced irrigation, SI reduced photosynthesis, resulting in lower starch content in both leaves and grains, and consequently, reduced yield (Dilkes et al., 2009). Additionally, AO prefers to allocate the increased carbon supply from leaf photosynthesis to leaf starch, rather than to grain formation and starch accumulation in the endosperm.

3.3. Starch multi-structures and digestibility

To further assess the effects of SI on the starch qualities, starches were extracted, and their molecular, crystalline and granular structures, as well as digestibility were characterized and discussed in the following sections.

3.3.1. Molecular structures

AAC results in Table 2 indicated that SI treatment resulted in a more pronounced reduction in AO (20 %) compared to NB (1.5 %). The decreased AAC was also reported in SI-treated winter wheat (Liang et al., 2021), indicating that SI treatment led to a reduction in AAC in both wheat and barley. AAC, measured by iodine complexation, reflects the length of glucan chains in AM and AM-like materials (Knutson, 2000). As AO barley starch is almost entirely composed of AM and AM-like material (Zhong et al., 2022), its AAC value of 114 % is attributed to a high proportion of long-chain AM molecules. The decreased AAC in AOSI likely suggested that SI shortened the AM chains.

The chain length distributions of debranched starch (molar based) were evaluated by HPAEC-PAD. Data in Fig. 3 and Table 2 indicated that SI treatment to AO resulted in increased amount of short AM side chains (DP $\leq$ 24) and a lower proportion of long AM side chains (DP $>$ 24) (Fig. 3 and Table 2), in line with its decreased AAC. In addition, both AO starches lacked chains with DP $>$ 40, likely due to their limited number of side chains, particularly long chains. In NB, SI decreased the content of AP chains with DP 12–36 while increasing the proportion of AP chains with DP $>$ 36 (Fig. 3 and Table 2). A decreased content in AP chains with DP 12–24 was also reported in SI treated wheat starch (Liang et al., 2021), indicating a distinct response of the AM-only genotype to SI treatment when compared with the medium-AM genotype.

H NMR spectra (Table 3) further demonstrated the limited branches in AO (1.7–1.9 %). SI treatment led to a decrease in the branching degree of NB. Short AP chains primarily form the branching regions of AP, while long AP chains provide the backbone structure (Bertoft, 2017). Therefore, the reduced branching degree in NBSI aligns with the decreased content of short AP chains (DP $\leq$ 36). In contrast, a slightly increased branching degree was observed in AOSI compared to AOWW, in line with the reductions in AAC and increased contents of shorter chains noted in the AM-like material, as discussed above.

3.3.2. Crystalline structures

WAXS profiles (Fig. S1) mainly displayed the typical A-type crystalline allomorph with two strong peaks at 2θ around 15° and 23°, an unresolved doublet at 2θ =17 and 18° for NBWW and NBSI, and a combination of B-type (at 2θ = 5.6°, 17° and 24°) and V-type (at 2θ = 7°, 13° and 20°) allomorph for AOWW and AOSI, in agreement with our previous study (Zhong et al., 2021). Notably, SI increased the relative crystallinity of both NB and AO (Table 3), consistent with a previous report (Song et al., 2017). In AO, this increase is likely attributed to an

Table 1
Grain yield, grain yield components, and total starch content of two barley genotypes upon two different irrigation methods[1].

Cultivar[2]	Irrigation treatment	Number of spikes	Grain number per spike	Thousand grain weight (g)	Grain yield per plant (g)	Total starch content (%)
NB	WW	72.7 ± 2.9^a	31.5 ± 2.7^a	49.1 ± 0.9^a	37.7 ± 0.5^a	49.1 ± 0.8^a
	SI	65.2 ± 2.9^b	31.9 ± 2.5^a	48.5 ± 0.6^a	33.3 ± 0.1^b	44.3 ± 1.6^b
AO	WW	71.0 ± 2.7^a	32.4 ± 2.3^a	35.7 ± 0.6^a	27.9 ± 0.3^a	31.1 ± 0.7^a
	SI	69.6 ± 2.5^a	32.2 ± 2.7^a	36.1 ± 0.3^a	26.8 ± 0.1^b	28.7 ± 0.9^b

[1] All data are means ±standard deviations. Values with different letters are significantly different at $p < 0.05$, $n = 3$.
[2] NB, Normal barley; AO, Amylose-only; SI, Supplemental irrigation; WW, Well-watered.

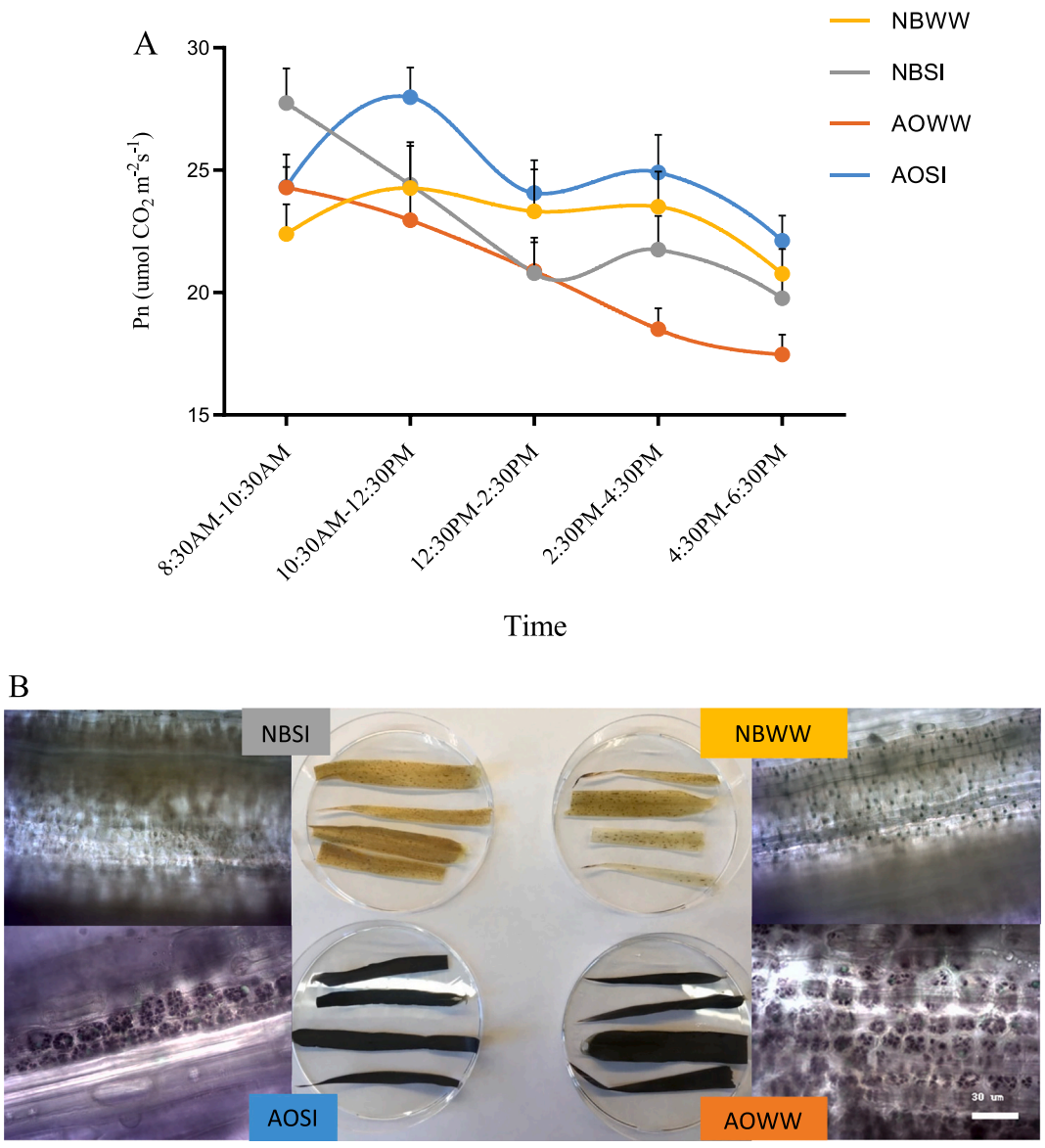

Fig. 2. Dynamic changes in flag-leaf photosynthesis (A) and visualization of leaf starch granules (B) at the anthesis stage (The abbreviations are the same as Fig. 1).

Table 2
AAC and chain length distributions of debranched starches from two barley genotypes upon two different irrigation methods[1].

Cultivar[2]	Irrigation treatment	AAC (%)	fa DP 6–12 (%)	fb_1 DP 13–24 (%)	fb_2 DP 25–36 (%)	fb_3 DP > 36 (%)
NB	WW	32.6 ± 0.1[a]	11.7 ± 0.8[a]	57.8 ± 3.1[a]	22.8 ± 1.6[a]	6.5 ± 1.6[a]
	SI	31.1 ± 1.0[b]	11.4 ± 1.0[a]	56.1 ± 0.6[a]	20.4 ± 0.6[b]	9.0 ± 1.3[a]
AO	WW	114.0 ± 12.0[a]	18.7 ± 0.8[b]	40.6 ± 2.3[b]	20.7 ± 0.1[a]	9.7 ± 1.7[a]
	SI	94.0 ± 4.7[b]	21.0 ± 0.2[a]	45.3 ± 0.6[a]	19.0 ± 0.1[b]	8.8 ± 0.1[a]

[1] All data are means ± standard deviations. Values with different letters are significantly different at $p < 0.05$, n = 3.
[2] NB, Normal barley; AO, Amylose-only; SI, Supplemental irrigation; WW, Well-watered.

elevated branching degree and a higher proportion of short side chains with DP < 24 induced by the SI treatment. Short side chains (DP < 36) are predominantly located in the crystalline nano-lamellae (Bertoft, 2017), with chains of DP 6–18 positively correlated with crystallinity (Zhong, Bertoft, Li, Blennow, & Liu, 2020). However, the decreased branching degree and unchanged side chains with DP < 24 induced in SI treated NB, suggested that the increased crystallinity may stem from other factors beyond molecular structural changes. A possible explanation is that SI enhances crystallinity by modifying the packing and/or alignment of double-helical segments during starch biosynthesis. Interestingly, SI has been shown to decrease crystallinity in wheat starches (Liang et al., 2021), suggesting that SI has different effects on the crystalline structure of starches depending on the botanical source.

3.3.3. *Granular structures*

The granular surface bonding order, as analyzed by FTIR (Table 3), showed that the SI treatments decreased the ratio of 1047/1022 cm^{-1} in both genotypes of starches, indicating that the structural ordering of the

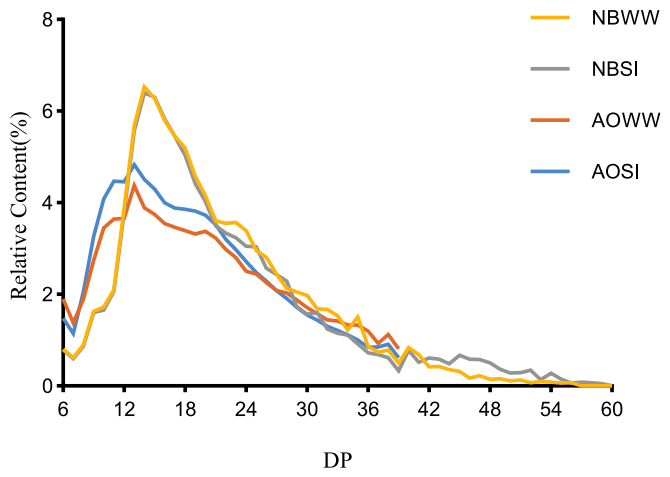

Fig. 3. Chain lengths distributions of debranched barley starches analyzed by HPAEC-PAD. The abbreviations are the same as Fig. 1.

starch granule surface was disrupted by SI (Kizil, Irudayaraj, & Seetharaman, 2002; Zhong et al., 2021). This result is opposite to the changes observed for crystallinity as determined WAXS (Fig. S2 and Table 3). Hence, in general, SI probably increased the internal structural ordering and decreased the ordering of outer layers of starch granules of barley. This apparent contradiction may reflect the asynchronous development of the internal layer and the granule surface during endosperm maturation. A previous study has reported similar observations in tuber crops, where during sweet potato tuber development, the crystallinity increased while the surface order did not change (Wang et al., 2024). The enhancement of internal crystallinity may originate from tighter packing of double helices or longer molecular chain arrangement, while the decrease in surface order may be caused by reduced external growth organization due to water deficiency in SI during grain expansion. To further explore this, starch granule formation during endosperm development needs be performed in the future.

Granular size distribution analysis in Table 3 and Fig.S2 showed that SI treatments significantly increased the specific surface area of both NB and AO (Table 3), in agreement with the changes observed for wheat starch (Liang et al., 2021). D (4,3) represents a pertinent metric related to the size distribution of starch granules. SI increased D (4,3) value of AO but had little effect on the NB. This suggests that, on the one hand, SI suppressed the accumulation of starch during endosperm development, as reflected by decreased total starch content, but on the other hand, SI stimulated the growth and development of individual starch granules in the endosperm demonstrated by increased granule size. SEM images (Fig.S3) revealed that SI had no effect on the morphology of NB and promoted the aggregation of granules accompanied by the formation of many small pores in AO, supported by the increased specific surface area in the samples.

3.3.4. Digestion properties

The *in vitro* digestion data (Table 4) revealed the effects of SI on the contents of rapidly digestible starch (RDS, 0–20 min), slowly digestible starch (SDS, 20–120 min), and resistant starch (RS, not digestible within 120 min). In NB, SI increased the RDS content while slightly reducing both SDS and RS, indicating enhanced enzymatic accessibility in SI-treated NB. In contrast, for AO, SI primarily increased SDS while reducing RS, suggesting that SI treatment could be a potential strategy for developing slowly-digestible AO-based food products. This may have practical significance for the development of low-glycemic index or sustained-release starch-based food products, especially in the context of health-focused grain applications. These findings indicate that SI enhanced the digestibility of both NB and AO, likely due to influence of SI on reducing the structural order of granular surfaces and on increasing the specific surface area (Table 3). Our previous study indicated that granular surface ordering structures affect starch digestion by regulating enzyme binding efficiency (Liang et al., 2023). While, higher available surface area facilitates diffusion and adsorption of enzymes (Dhital, Shrestha, & Gidley, 2010). Therefore, less ordered surface structure and larger area of surface facilitates enzyme binding and absorption, thereby accelerating digestion. These results also highlight that starch digestibility can be regulated by modulating surface order and area through SI treatment, by inducing the formation of distinct enzymatically sensitive regions. Additionally, AM molecules undergo structural reorganization during enzymatic hydrolysis (Shrestha et al., 2012), and shorter AM chains have been suggested to form hydrolytically resistant, densely packed aggregates more efficiently than longer chains (Zhong et al., 2022). As discussed in Section 3.3.1, the increased generation of short AM chains (DP $\leq$ 24) for AO under SI treatment may have the capability to reorganize to a more ordered structure during the hydrolysis, thereby contributing to the observed increase in SDS in AO. However, SI has been reported to increase RS in wheat starch (Liang et al., 2021), further highlighting the diverse impacts of SI on starch digestibility, depending on the botanical origin of the samples.

3.4. Gene expression

Expression of 7 starch biosynthesis-related genes during endosperm development from 0 to 35 days after anthesis (Fig. 4) revealed that SI treatment upregulated Granule-Bound Starch Synthase I (*GBSSI*), Starch Synthase III (*SSIII*), and Starch Branching Enzyme IIb (*SBEIIb*) while downregulating of Isoamylase (*ISA*). Notably, SI had varying effects on the expression levels of *SSI*, *SSIIa*, and *SBEI*, as discussed in the following sections. These results indicate that reduced irrigation in SI can

Table 4
In vitro digestibility of starches from two barley genotypes upon two different irrigation methods.[1]

Cultivar[2]	Irrigation treatment	RDS (%)	SDS (%)	RS (%)
NB	WW	35.2 ± 1.3^{b}	44.9 ± 1.7^{a}	20.4 ± 1.8^{a}
	SI	38.3 ± 1.4^{a}	43.6 ± 2.7^{a}	17.3 ± 2.9^{a}
AO	WW	33.6 ± 0.6^{a}	19.2 ± 1.3^{b}	47.5 ± 1.3^{a}
	SI	34.1 ± 0.7^{a}	23.7 ± 0.8^{a}	41.2 ± 1.4^{b}

[1] All data are means ±standard deviations. Values with different letters are significantly different at $p < 0.05$, $n = 3$.
[2] NB, Normal barley; AO, Amylose-only; SI, Supplemental irrigation; WW, Well-watered.

Table 3
Branching degree, granular surface structure, crystallinity, and granular size related parameters of starches from two barley genotypes upon two different irrigation methods[1].

Cultivar[2]	Irrigation treatment	Branching degree (%)	Relative crystallinity (%)	1047/1022 cm^{-1}	Specific surface area (m^2/kg)	D (4,3)
NB	WW	3.6 ± 0.0^{a}	21.9 ± 1.5^{b}	0.62 ± 0.01^{a}	416 ± 29^{b}	17.7 ± 0.8^{a}
	SI	3.5 ± 0.0^{b}	23.8 ± 0.0^{a}	0.41 ± 0.03^{b}	525 ± 22^{a}	17.8 ± 2.2^{a}
AO	WW	1.7 ± 0.0^{b}	22.0 ± 0.8^{b}	0.58 ± 0.04^{a}	379 ± 2^{b}	21.3 ± 0.1^{b}
	SI	1.9 ± 0.0^{a}	23.4 ± 0.8^{a}	0.54 ± 0.02^{a}	391 ± 3^{a}	22.4 ± 0.1^{a}

[1] All data are means ±standard deviations. Values with different letters are significantly different at $p < 0.05$, n = 3.
[2] NB, Normal barley; AO, Amylose-only; SI, Supplemental irrigation; WW, Well-watered.

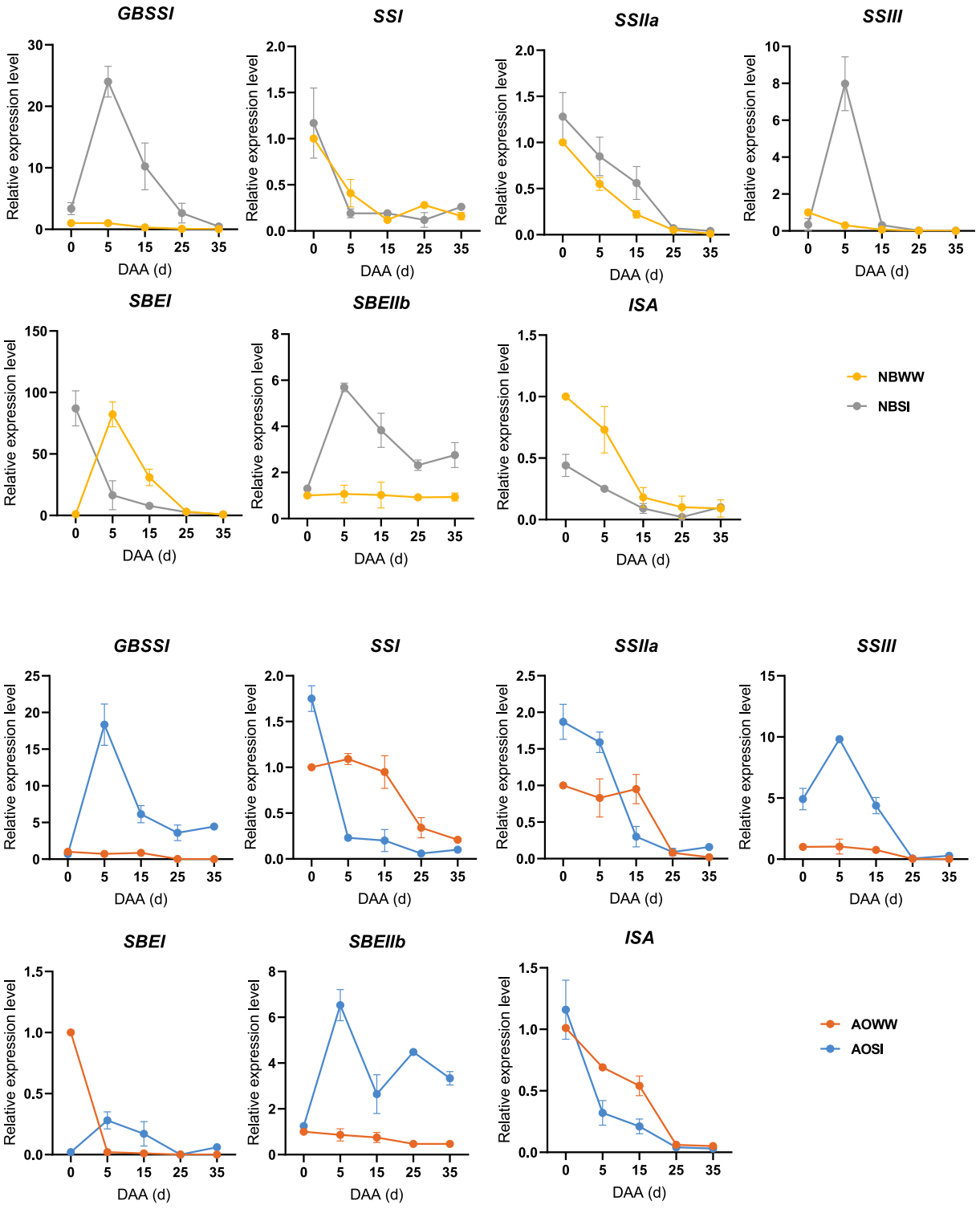

Fig. 4. The relative expression levels of starch biosynthesis-related genes during endosperm development of barley grains for NB and AO genotypes (The abbreviations are the same as Fig. 1. DAA: Days after anthesis).

modulate starch structure and properties by regulating these starch synthetic genes.

(I)The expression level of *SSI* remained relatively unchanged in NB, whereas in SI-treated AO, its expression decreased. *SSI* primarily synthesizes chains with DP 8–12 from shorter chains of DP 4–7 (Cuesta-Seijo et al., 2016). These results explain the absence of change in proportion of shorter chains (DP $\leq$ 12) of NBSI (Table 2); however, they are opposite to the increased proportion of these chains observed in the AOSI samples. The increased short AM chains with DP $\leq$ 12 is likely attributed to increased *SSI* enzymatic activity for AO under SI treatment, which needs to be investigated in the future.

(II)The expression level of *SSIIa* increased in NBSI compared to NBWW. Similarly, in AOSI, *SSIIa* expression increased at 0–5 days after anthesis compared to AOWW but subsequently decreased. Previous studies have shown that *SSIIa*-null barley mutants exhibit a lower content of AP chains with DP 35–70 (Yang et al., 2022), suggesting that

SSIIa plays a role in synthesizing long AP chains. Accordingly, the increased *SSIIa* expression in NBSI (Fig. 4) led to a slightly higher content of AP long chains with DP > 36 in NB (Table 2). Conversely, the decreased *SSIIa* expression was associated with a lower content of chains with DP > 36 in AO. However, *SSIIa* has also been reported to be responsible for synthesizing chains with DP 13–28 in barley (Yang et al., 2022). Unexpectedly, an increased content of side chains with DP 13–24 was observed in AOSI, despite the decreased *SSIIa* expression during later endosperm development of grains. This result may be explained by the high enzymatic activity of *SSIIa* protein. To clarify this, further investigations are required.

(III) SI decreased the expression level of *SBEI* in NB but increased it in AO throughout the endosperm development period, which might explain the observed decrease in branching degree of NB and increase in branching degree of AO (Table 3). Additionally, SI increased the expression level of *GBSSI* in both NB and AO, which is unexpected given the decreased AAC in these two starches. Notably, three *SBE*s were silenced in the AO line (Carciofi et al., 2012), The upregulation of *SBEI* and *SBEIIb* in AOSI induced increased branching degree, thereby decreasing the AAC. Similarly, the higher expression of *SBEIIb* in NBSI also resulted in reduced AAC, despite the downregulation of *SBEI*.

4. Conclusion

The effects of SI on starch structure, *in vitro* digestibility and biosynthesis were investigated in this study using two barley genotypes: NB and AO. Compared to WW condition, SI reduced grain yield and starch content in both genotypes, with a more pronounced decline in NB than in AO. Additionally, SI decreased photosynthetic capacity in NB but increased it in AO, corroborated by variations in the number of starch granules in leaves. In NB, SI increased the proportion of long AP chains with DP >36, while in AO, it enhanced the content of short AM side chains (DP ≤ 24). SI also upregulated S*SIIa* in NB and downregulated *SSI* and *SSIIa* in AO. Moreover, SI led to reductions in AAC and starch granular surface structural ordering, and increases in starch granule size and crystallinity in both genotypes. Furthermore, SI promoted starch digestibility, specifically elevating RDS in NB and SDS in AO, likely due to reduced surface ordered degrees and increased surface area. These results highlighted the diverse impacts of SI on starch structure and digestibility among different genotypes, supporting our hypothesis. This can be attributed to the suppression of all *SBE* genes in AO, which led to distinct pleiotropic changes in the expression patterns of starch synthetic genes, such as *SSI*, *SSIIa*, and *SBEI*, under the same SI treatment compared to its mother counterpart, NB. Furthermore, comparison with our previous study on normal wheat starch indicated that botanical origin also influences the effects of SI on these properties.

In summary, this study showed that barley genotypes respond differently to SI in both yield and starch qualities: AO, with suppression of all *SBE* genes, showed increased content of short AM chains, crystallinity, and SDS under SI, while NB exhibited larger reductions in the yield and starch content, reduced surface order, and increased RDS. These findings indicate that irrigation management interacts with intrinsic starch metabolic pathways to influence starch quality in a genotype-dependent manner. Notably, our results also suggest that irrigation strategies taking into account specific genotypes, can help modulate grain functional traits under water-saving management, which offers valuable guidance for breeding and agronomic practices to optimize nutritional quality in the face of a changing climate. However, it should be noted that the present study utilized only a single starch biosynthesis RNAi suppressor line (AO) in comparison with a wild-type control (NB). The AO line, which contains only AM and AM-like molecules due to suppression of all *SBE* genes, was selected as an extreme contrasting genotype to investigate how irrigation interacts with altered starch biosynthetic pathways. As a result, this study does not provide a comprehensive mechanistic understanding of how irrigation regulates starch metabolism. Nevertheless, the current findings represent an important initial step toward elucidating genotype × irrigation interactions in starch biosynthesis. Future research should incorporate multiple starch biosynthesis mutants targeting different enzymes (*e.g.*, SBE, SS, or starch debranching enzyme isoforms), employ integrative approaches such as transcriptomics and metabolomics, and conduct multi-year field trials to validate and extend these findings.

CRediT authorship contribution statement

Wenxin Liang: Writing – original draft, Validation, Software, Methodology, Investigation, Conceptualization. **Klaus Herburger:** Writing – review & editing. **Ke Guo:** Methodology, Investigation. **Jacob Judas Kain Kirkensgaard:** Writing – review & editing, Methodology. **Kim Henrik Hebelstrup:** Resources. **Staffan Persson:** Writing – review & editing. **Sheng Chen:** Writing – review & editing. **Yuyue Zhong:** Writing – review & editing, Supervision, Project administration. **Andreas Blennow:** Writing – review & editing, Supervision, Resources. **Li Ding:** Writing – review & editing, Writing – original draft, Methodology, Investigation.

Declaration of competing interest

The authors declare that they have no known competing financial interests or personal relationships that could have appeared to influence the work reported in this paper.

Acknowledgements

Wenxin Liang gratefully acknowledges financial support from the China Scholarship Council (CSC) (Grant No. 201906300091). The authors extend their sincere appreciation to Theodor E. Bolsterli and the plant facilities team at PLEN, University of Copenhagen, for their invaluable assistance in greenhouse plant cultivation. We also thank Wen Shao for insightful discussions and support throughout the study.

Appendix A. Supplementary data

Supplementary data to this article can be found online at https://doi.org/10.1016/j.carbpol.2025.124378.

Data availability

Data will be made available on request.

References

Ambavaram, M. M., Basu, S., Krishnan, A., Ramegowda, V., Batlang, U., Rahman, L., & Pereira, A. (2014). Coordinated regulation of photosynthesis in rice increases yield and tolerance to environmental stress. *Nature Communications, 5*, 5302.

Asare, E. K., Jaiswal, S., Maley, J., Baga, M., Sammynaiken, R., Rossnagel, B. G., & Chibbar, R. N. (2011). Barley grain constituents, starch composition, and structure affect starch in vitro enzymatic hydrolysis. *Journal of Agricultural and Food Chemistry, 59*(9), 4743–4754.

Bertoft, E. (2017). Understanding starch structure: Recent progress. *Agronomy, 7*(3), Article 56.

Blennow, A., Bay-Smidt, A. M., Wischmann, B., Olsen, C. E., & Møller, B. L. (1998). The degree of starch phosphorylation is related to the chain length distribution of the neutral and the phosphorylated chains of amylopectin. *Carbohydrate Research, 307*(1), 45–54.

Carciofi, M., Blennow, A., Jensen, S. L., Shaik, S. S., Henriksen, A., Buléon, A., & Hebelstrup, K. H. (2012). Concerted suppression of all starch branching enzyme genes in barley produces amylose-only starch granules. *BMC Plant Biology, 12*(1), 223.

Cuesta-Seijo, J. A., Nielsen, M. M., Ruzanski, C., Krucewicz, K., Beeren, S. R., Rydhal, M. G., & Palcic, M. M. (2016). In vitro biochemical characterization of all barley endosperm starch synthases. *Frontiers in Plant Science, 6*.

Dai, Z., Li, Y., Zhang, H., Yan, S., & Li, W. (2016). Effects of irrigation schemes on the characteristics of starch and protein in wheat (Triticum aestivumL.). *Starch - Stärke, 68*(5–6), 454–461.

Dhital, S., Shrestha, A. K., & Gidley, M. J. (2010). Relationship between granule size and in vitro digestibility of maize and potato starches. *Carbohydrate Polymers, 82*(2), 480–488.

Dietz, K. J., Zorb, C., & Geilfus, C. M. (2021). Drought and crop yield. *Plant Biololgy (Stuttg), 23*(6), 881–893.
Dilkes, B. P., Hayano-Kanashiro, C., Calderón-Vázquez, C., Ibarra-Laclette, E., Herrera-Estrella, L., & Simpson, J. (2009). Analysis of gene expression and physiological responses in three Mexican maize landraces under drought stress and recovery irrigation. *PLoS One, 4*(10), Article e7531.
Ding, L., Liang, W., Qu, J., Persson, S., Liu, X., Herburger, K., & Zhong, Y. (2023). Effects of natural starch-phosphate monoester content on the multi-scale structures of potato starches. *Carbohydrate Polymers, 310*, Article 120740.
Dogan, E. (2019). Effect of supplemental irrigation on vetch yield components. *Agricultural Water Management, 213*, 978–982.
Fahong, W., Xuqing, W., & Sayre, K. (2004). Comparison of conventional, flood irrigated, flat planting with furrow irrigated, raised bed planting for winter wheat in China. *Field Crops Research, 87*(1), 35–42.
Fonteyne, S., Flores García, Á., & Verhulst, N. (2021). Reduced water use in barley and maize production through conservation agriculture and drip irrigation. *Frontiers in Sustainable Food Systems, 5*.
Goldstein, A., Annor, G., Putaux, J.-L., Hebelstrup, K. H., Blennow, A., & Bertoft, E. (2016). Impact of full range of amylose contents on the architecture of starch granules. *International Journal of Biological Macromolecules, 89*, 305–318.
Gowing, J., & Ejieji, C. (2001). Real-time scheduling of supplemental irrigation for potatoes using a decision model and short-term weather forecasts. *Agricultural Water Management, 47*(2), 137–153.
Guo, Z., Yu, Z., Wang, D., Shi, Y., & Zhang, Y. (2014). Photosynthesis and winter wheat yield responses to supplemental irrigation based on measurement of water content in various soil layers. *Field Crops Research, 166*, 102–111.
Honda, S., Ohkubo, S., San, N. S., Nakkasame, A., Tomisawa, K., Katsura, K., … Adachi, S. (2021). Maintaining higher leaf photosynthesis after heading stage could promote biomass accumulation in rice. *Scientific Reports, 11*(1), Article 7579.
Ippolito, J. A., Bjorneberg, D., Stott, D., & Karlen, D. (2017). Soil Quality Improvement through Conversion to Sprinkler Irrigation. *Soil Science Society of America Journal, 81*(6), 1505–1516.
Jian, H., Gao, Z., Guo, Y., Xu, X., Li, X., Yu, M., & Du, X. (2024). Supplemental irrigation mitigates yield loss of maize through reducing canopy temperature under heat stress. *Agricultural Water Management, 299*, Article 108888.
Kizil, R., Irudayaraj, J., & Seetharaman, K. (2002). Characterization of irradiated starches by using FT-Raman and FTIR spectroscopy. *Journal of Agricultural and Food Chemistry, 50*(14), 3912–3918.
Knutson, C. A. (2000). Evaluation of variations in amylose–iodine absorbance spectra. *Carbohydrate Polymers, 42*(1), 65–72.
Liang, W., Blennow, A., Herburger, K., Zhong, Y., Wen, X., Liu, Y., & Liao, Y. (2021). Effects of supplemental irrigation on winter wheat starch structure and properties under ridge-furrow tillage and flat tillage. *Carbohydrate Polymers, 270*, Article 118310.
Liang, W., Ding, L., Guo, K., Liu, Y., Wen, X., Kirkensgaard, J. J. K., … Zhong, Y. (2023). The relationship between starch structure and digestibility by time-course digestion of amylopectin-only and amylose-only barley starches. *Food Hydrocolloids, 139*, Article 108491.
Oweis, T., Hachum, A., & Pala, M. (2004). Lentil production under supplemental irrigation in a Mediterranean environment. *Agricultural Water Management, 68*(3), 251–265.
Passioura, J. B. (2006). The perils of pot experiments. *Functional Plant Biology, 33*(12), 1075–1079.
Samarah, N. H., Alqudah, A. M., Amayreh, J. A., & McAndrews, G. M. (2009). The Effect of Late-terminal Drought Stress on Yield Components of Four Barley Cultivars. *Journal of Agronomy and Crop Science, 195*(6), 427–441.
Shrestha, A. K., Blazek, J., Flanagan, B. M., Dhital, S., Larroque, O., Morell, M. K., & Gidley, M. J. (2012). Molecular, mesoscopic and microscopic structure evolution during amylase digestion of maize starch granules. *Carbohydrate Polymers, 90*(1), 23–33.
Song, Z., Zhong, Y., Tian, W., Zhang, C., Hansen, A. R., Blennow, A., & Guo, D. (2020). Structural and functional characterizations of α-amylase-treated porous popcorn starch. *Food Hydrocolloids, 108*, Article 105606.
Wang, D., Yu, Z., & White, P. J. (2013). The effect of supplemental irrigation after jointing on leaf senescence and grain filling in wheat. *Field Crops Research, 151*, 35–44.
Wang, H., Feng, Y., Guo, K., Shi, L., Xu, X., & Wei, C. (2024). Structural, thermal, pasting and digestion properties of starches from developing root tubers of sweet potato. *Foods, 13*(7), Article 1103.
Wickramasinghe, H. A. M., Blennow, A., & Noda, T. (2009). Physico-chemical and degradative properties of in-planta re-structured potato starch. *Carbohydrate Polymers, 77*(1), 118–124.
Song, X., Zhang, M., Wu, X., Zhao, C., Shi, J., Zhang, Y., Liu, X., & Cai, R. (2017). Effects of drought stress on wheat endosperm starch structure and physicochemical properties of different Varieties. *Scientia Agricultura Sinica, 50*(2), 260–271.
Yang, Q., Ding, J., Feng, X., Zhong, X., Lan, J., Tang, H., & Jiang, Q. (2022). Editing of the starch synthase IIa gene led to transcriptomic and metabolomic changes and high amylose starch in barley. *Carbohydrate Polymers, 285*, Article 119238.
Yu, X., Li, B., Wang, L., Chen, X., Wang, W., Gu, Y., & Xiong, F. (2016). Effect of drought stress on the development of endosperm starch granules and the composition and physicochemical properties of starches from soft and hard wheat. *Journal of the Science of Food and Agriculture, 96*(8), 2746–2754.
Zhong, Y., Bertoft, E., Li, Z., Blennow, A., & Liu, X. (2020). Amylopectin starch granule lamellar structure as deduced from unit chain length data. *Food Hydrocolloids, 108*, Article 106053.
Zhong, Y., Keeratiburana, T., Kain Kirkensgaard, J. J., Khakimov, B., Blennow, A., & Hansen, A. R. (2021). Generation of short-chained granular corn starch by maltogenic alpha-amylase and transglucosidase treatment. *Carbohydrate Polymers, 251*, Article 117056.
Zhong, Y., Li, Y., Qu, J., Zhang, X., Seytahmetovna, S. A., Blennow, A., & Guo, D. (2021). Structural features of five types of maize starch granule subgroups sorted by flow cytometry. *Food Chemistry, 356*, Article 129657.
Zhong, Y., Qu, J. Z., Liu, X., Ding, L., Liu, Y., Bertoft, E., & Blennow, A. (2022). Different genetic strategies to generate high amylose starch mutants by engineering the starch biosynthetic pathways. *Carbohydrate Polymers, 287*, Article 119327.
Zhong, Y., Tai, L., Blennow, A., Ding, L., Herburger, K., Qu, J., … Liu, X. (2022). High-amylose starch: Structure, functionality and applications. *Critical Reviews in Food Science and Nutrition*, 1–23.
Zhong, Y., Tian, Y., Liu, X., Ding, L., Kirkensgaard, J. J. K., Hebelstrup, K., & Blennow, A. (2021). Influence of microwave treatment on the structure and functionality of pure amylose and amylopectin systems. *Food Hydrocolloids, 119*, Article 106856.